

# Electronic correlations at the $\alpha$ - $\gamma$ structural phase transition in paramagnetic iron

I. Leonov,<sup>1</sup> A. I. Poteryaev,<sup>2,3</sup> V. I. Anisimov,<sup>2</sup> and D. Vollhardt<sup>1</sup>

<sup>1</sup>Theoretical Physics III, Center for Electronic Correlations and Magnetism,  
Institute of Physics, University of Augsburg, Augsburg 86135, Germany

<sup>2</sup>Institute of Metal Physics, S. Kovalevskoy St. 18, 620219 Yekaterinburg GSP-170, Russia

<sup>3</sup>Institute of Quantum Materials Science, 620107 Yekaterinburg, Russia

We compute the equilibrium crystal structure and phase stability of iron at the  $\alpha$ (bcc)- $\gamma$ (fcc) phase transition as a function of temperature, by employing a combination of *ab initio* methods for calculating electronic band structures and dynamical mean-field theory. The magnetic correlation energy is found to be an essential driving force behind the  $\alpha$ - $\gamma$  structural phase transition in paramagnetic iron.

PACS numbers: 71.10.-w, 71.27.+a

The properties of iron have fascinated mankind for several thousand years already. Indeed, iron has been an exceptionally important material for the development of modern civilization and its technologies. Nevertheless, even today many properties of iron, e.g., at high pressures and temperatures, are still not sufficiently understood. Therefore iron remains at the focus of active research.

At low pressures and temperatures iron crystallizes in a body-centered cubic (bcc) structure, referred to as  $\alpha$ -iron or ferrite; see Fig. 1. In particular, at ambient pressure iron is ferromagnetic, with an anomalously high Curie temperature of  $T_C \sim 1043$  K. Upon heating, iron exhibits several structural phase transformations [1, 2]: at  $\sim 1185$  K to the face-centered cubic (fcc) phase ( $\gamma$ -iron or austenite), and at  $\sim 1670$  K again to a bcc structure ( $\delta$ -iron). At high pressure iron becomes paramagnetic with a hexagonal close packed structure ( $\epsilon$ -iron).

Density functional theory (DFT) in the local spin density approximation gives a quantitatively accurate description of the ordered magnetic moment and the spin stiffness of bcc-Fe [3], but predicts the nonmagnetic fcc structure to be more stable than the observed ferromagnetic bcc phase [4]. Only if the spin polarized generalized-gradient approximation (GGA) [5] is applied does one obtain the correct ground state properties of iron [6].

Stoner theory of ferromagnetism [7] can give a qualitatively correct description of several magnetic and structural properties of iron, but predicts a simultaneous magnetic and structural change at the bcc-fcc phase transition with a local moment collapse while, in fact, the bcc-fcc phase transition occurs  $\sim 200$  K above  $T_C$ ; see Fig. 1. Clearly, to account for finite temperature effects of itinerant magnets one requires a formalism which takes into account the existence of local moments above  $T_C$ . While the spin-fluctuation theory, which describes the paramagnetic state above  $T_C$  as a collection of disordered moments, gives an overall good qualitative explanation of the pressure-temperature phase diagram of iron [8] it fails to provide a reasonably quantitative description and, in particular, predicts the bcc-fcc phase transition to occur

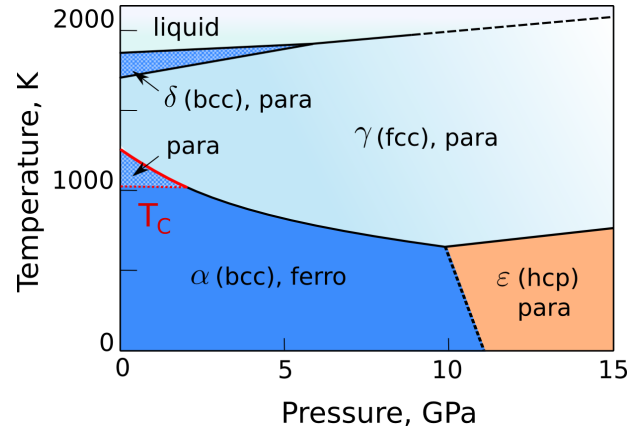


FIG. 1: (color online) Schematic temperature-pressure phase diagram of iron (see text).

below  $T_C$ .

The LDA+DMFT computational scheme [9], a combination of the DFT in the local density approximation (LDA) with dynamical mean-field theory (DMFT) [10], goes beyond the approaches discussed above since it explicitly includes many-body effects in a non-perturbative and thermodynamically consistent way. LDA+DMFT was already used to calculate the magnetization and the susceptibility of  $\alpha$ -iron as a function of the reduced temperature  $T/T_C$  [11]. The calculations gave overall good agreement with experimental data. The problem has been recently revisited by Katanin *et al.* [12] who found that the formation of local moments in paramagnetic  $\alpha$ -Fe is governed by the  $e_g$  electrons and is accompanied by non-Fermi liquid behavior. This supports the results obtained with the  $s$ - $d$  model for the  $\alpha$ -phase of iron [13].

A recent implementation of the LDA/GGA+DMFT scheme in plane-wave pseudopotentials [14, 15] now allows one to investigate correlation induced lattice transformations such as the cooperative Jahn-Teller distortion in  $\text{KCuF}_3$  and  $\text{LaMnO}_3$ . The method was not yet used to study structural phase transitions in a paramagnetic correlated electron system with temperature (or pressure)

involving a change of symmetry. This will be the goal of the present investigation.

In this Letter we employ the above-mentioned implementation of the LDA/GGA+DMFT scheme [14, 15] to explore the structural and magnetic properties of paramagnetic iron at finite temperatures. In particular, we will study the origin of the  $\alpha$ - $\gamma$  structural phase transformation, and the importance of electronic correlations for this transition. We first compute the nonmagnetic GGA electronic structure of iron [16]. To model the bcc-fcc phase transition we employ the Bain transformation path which is described by a single structural parameter  $c/a$ , the uniaxial deformation along [001] axis, with  $c/a = 1$  for the bcc and  $c/a = \sqrt{2}$  for the fcc structure. Here the lattice volume is kept at the experimental volume of  $\alpha$ -iron ( $a = 2.91$  Å) [2] in the vicinity of the bcc-fcc phase transition, while the  $c/a$  ratio is changed from 0.8 to 1.6. Overall, the GGA results qualitatively agree with previous band-structure calculations [6]. In particular, the nonmagnetic GGA yields the fcc structure to be more energetically favorable than the bcc one (see Fig. 2).

Next we apply the GGA+DMFT approach [14, 15] to determine the structural phase stability of iron. For the partially filled Fe  $sd$  orbitals we construct a basis of atomic-centered symmetry-constrained Wannier functions [15]. The corresponding first-principles multiband Hubbard Hamiltonian has the form

$$\hat{H} = \hat{H}_{\text{GGA}} + \frac{1}{2} \sum_{imm',\sigma\sigma'} U_{mm'}^{\sigma\sigma'} \hat{n}_{im\sigma} \hat{n}_{im'\sigma'} - \hat{H}_{\text{DC}} \quad (1)$$

where  $\hat{n}_{im\sigma} = \hat{c}_{im\sigma}^\dagger \hat{c}_{im\sigma}$  and  $\hat{c}_{im\sigma}^\dagger$  ( $\hat{c}_{im\sigma}$ ) creates (destroys) an electron with spin  $\sigma$  in the Wannier orbital  $m$  at site  $i$ . Here  $\hat{H}_{\text{GGA}}$  is the effective low-energy Hamiltonian in the basis of Fe  $sd$  Wannier orbitals. The second term on the right-hand side of Eq. 1 describes the Coulomb interaction between Fe  $3d$  electrons in the density-density approximation. It is expressed in terms of the average Coulomb repulsion  $U$  and Hund's rule exchange  $J$ . In this calculation we use  $U = 1.8$  eV which is within the theoretical and experimental estimations  $\sim 1 - 2$  eV and  $J = 0.9$  eV [17]. Further,  $\hat{H}_{\text{DC}}$  is a double counting correction which accounts for the electronic interactions already described by the GGA (see below).

In order to identify correlation induced structural transformations, we calculate [14] the total energy as

$$E = E_{\text{GGA}}[\rho] + \langle \hat{H}_{\text{GGA}} \rangle - \sum_{m,k} \epsilon_{m,k}^{\text{GGA}} + \frac{1}{2} \sum_{imm',\sigma\sigma'} U_{mm'}^{\sigma\sigma'} \langle \hat{n}_{im\sigma} \hat{n}_{im'\sigma'} \rangle - E_{\text{DC}}, \quad (2)$$

where  $E_{\text{GGA}}[\rho]$  denotes the total energy obtained by GGA. Here  $\langle \hat{H}_{\text{GGA}} \rangle$  is evaluated as the thermal average of the GGA Wannier Hamiltonian. The third term

on the right-hand side of Eq. (2) is the sum of the Fe  $sd$  valence-state eigenvalues. The interaction energy, the 4-th term on the right-hand side of Eq. (2),  $\langle \hat{n}_{im\sigma} \hat{n}_{im'\sigma'} \rangle$  which is calculated in DMFT. The double-counting correction  $E_{\text{DC}} = \frac{1}{2} \sum_{imm',\sigma\sigma'} U_{mm'}^{\sigma\sigma'} \langle \hat{n}_{im\sigma} \rangle \langle \hat{n}_{im'\sigma'} \rangle$  corresponds to the average Coulomb repulsion between electrons in the Fe  $3d$  Wannier orbitals calculated from the self-consistently determined local occupancies [18].

To solve the realistic many-body Hamiltonian (1) within DMFT we employ quantum Monte Carlo (QMC) simulations with the Hirsch-Fye algorithm [19]. The calculations for iron are performed along the Bain transformation path as a function of the reduced temperature  $T/T_C$ . Here  $T_C$  corresponds to the temperature where the spin polarization in the self-consistent GGA+DMFT solution vanishes. We obtain  $T_C \sim 1600$  K which, given the local nature of the DMFT approach, is in reasonable agreement with the experimental value of 1043 K and also with earlier LDA+DMFT calculations [11]. We find that  $T_C$  depends sensitively on the lattice distortion  $c/a$ . It has a maximum value for the bcc ( $c/a = 1$ ) structure and decreases rapidly for other values. In particular, for all temperatures considered here the fcc phase remains paramagnetic.

In Fig. 2 we show the variation of the total energy of paramagnetic iron with temperature along the bcc-fcc Bain transformation path. The result exhibits two well-defined energy minima at  $c/a = 1$  (at low temperature) and  $c/a = \sqrt{2}$  (at high temperature), corresponding to the bcc and fcc structures, respectively. We find that for decreasing temperature the inclusion of the electronic correlations among the partially filled Fe  $3d$  states considerably reduces the total energy difference between the  $\alpha$  and  $\gamma$  phases. In particular, the bcc-to-fcc structural phase transition is found to take place at  $T_{\text{struct}} \sim 1.3 T_C$ , i.e., well above  $T_C$  [20]. Our result for  $\Delta T \equiv T_{\text{struct}} - T_C$ , the difference between the temperatures at which the magnetic transition and the structural phase transition occur, is in remarkable agreement with the experimental result of  $\Delta T \sim 200$  K. This finding differs from conventional band-structure calculations which predict the magnetic and structural phase transition to occur simultaneously. Both  $T_{\text{struct}}$  and  $T_C$  vary sensitively with the value of the Coulomb repulsion  $U$  employed in GGA+DMFT calculation. We find that  $T_{\text{struct}}$  increases for increasing  $U$  values, whereas  $T_C$  decreases, in agreement with the Kugel-Khomskii theory [21].

In addition, we performed LDA+DMFT calculations to determine the phase stability of iron at the bcc-fcc phase transition as a function of temperature. In contrast to the standard band structure approach where it is essential that the spin-polarized GGA is used to obtain the correct ground state properties of iron, we find that both the LDA+DMFT and GGA+DMFT schemes give qualitatively similar results. In particular, both schemes find the bcc-to-fcc structural phase transition at  $\sim 1.3 T_C$ ,

TABLE I: Calculated lattice constant  $a$  for the bcc lattice, volume  $V$  and bulk modulus  $B$  for the equilibrium phase of paramagnetic iron as a function of  $T/T_C$ .

$T/T_C$	Eq. phase	$a$ , Å	$V$ , au <sup>3</sup>	$B$ , Mbar
0 (GGA)	bcc	2.757	70.71	2.66
	fcc	2.737	69.20	2.82
0.9	bcc	2.880	80.64	1.48
1.2	bcc	2.883	80.84	1.50
1.4	fcc	2.861	79.03	1.61
1.8	fcc	2.862	79.13	1.59
Exp[1, 2, 22]	bcc/fcc	2.88-2.91		1.62-1.76

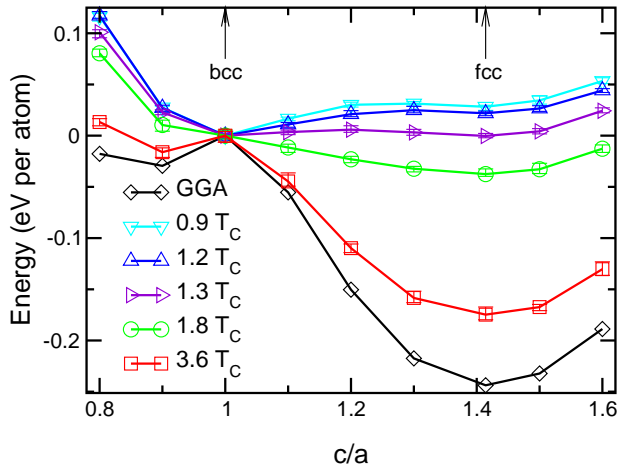


FIG. 2: (color online) Variation of the total energy of paramagnetic iron obtained by GGA and GGA+DMFT(QMC) for different temperatures. The total energy is calculated along the bcc-fcc Bain transformation path with constant volume ( $a = 2.91$  Å for the bcc phase). Error bars indicate the statistical error of the DMFT(QMC) calculations.

i.e., well above the magnetic transition. Explanations of the bcc-fcc structural phase transition and the fact that  $T_{\text{struct}} \neq T_C$  obviously need to go beyond conventional band structure theories. This clearly demonstrates the crucial importance of the electronic correlations among the partially filled Fe 3d states.

Next we perform a structural optimization and compute the equilibrium volume and the corresponding bulk modulus of paramagnetic iron (see Table I). The bulk modulus is calculated as the derivative of the total energy as a function of volume. We find that at the bcc-fcc phase transition the equilibrium lattice volume simultaneously shrinks by  $\sim 2\%$ , a result which is in good agreement with the experimental value of  $\sim 1\%$  [1]. The volume reduction is accompanied by an increase of the calculated bulk modulus. Overall, the equilibrium volume and bulk modulus computed by GGA+DMFT agree well with the experimental data [1, 2, 22].

Finally we compute the square of the instantaneous local moment  $\langle m_z^2 \rangle = \langle (\sum_m [\hat{n}_{m\uparrow} - \hat{n}_{m\downarrow}])^2 \rangle$  of paramagnetic iron for the distortions  $c/a$  considered here. In

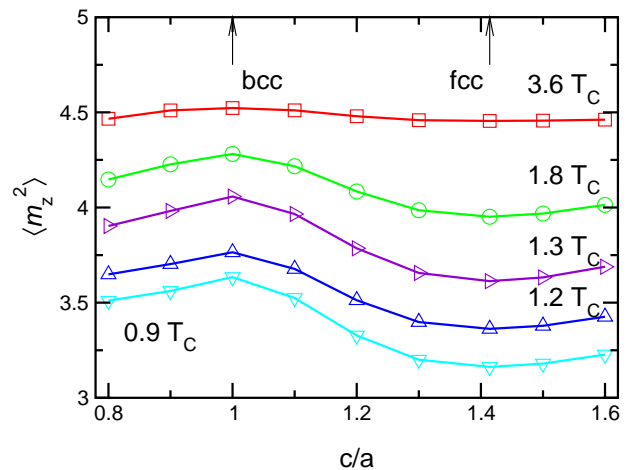


FIG. 3: (color online) Variation of the square of the local magnetic moment calculated by GGA+DMFT for paramagnetic iron.

Fig. 3 we show the result plotted for various temperatures. At low temperatures, the squared local moment depends quite strongly on the value of  $c/a$ , and is maximal in the bcc and minimal in the fcc phase, respectively. As expected, above  $T_C$ , the square local moment gradually increases with temperature and becomes essentially independent of  $c/a$ , as indicated by the curve for  $T = 3.6 T_C$  in Fig. 3 (we note that this is only a hypothetical curve since at such an elevated temperatures iron is already in its liquid state). This finding has important implications for our understanding of the actual driving force behind the bcc-to-fcc paramagnetic phase transition. For this we note that the squared local moment  $\langle m_z^2 \rangle$  determines the magnetic correlation energy  $-\frac{1}{4}I\langle m_z^2 \rangle$ , which is an essential part [23] of the total correlation energy of the Hamiltonian (1). At high temperatures, when the local moment is almost independent of  $c/a$  and the GGA+DMFT approach finds the fcc phase to be stable, the contribution of the magnetic correlation energy to the bcc-fcc total energy difference is seen to be negligible. This changes markedly when the temperature is lowered. Namely, upon cooling the contribution of the magnetic correlation energy gradually increases and becomes strong enough to overcome the DMFT kinetic energy loss  $E_{kin} = E_{GGA}[\rho] + \langle \hat{H}_{GGA} \rangle - \sum_{m,k} \epsilon_{m,k}^{GGA}$  for the bcc phase as compared with the fcc phase. Thereby the bcc phase with its larger value of the local moment is stabilized at  $T < 1.3 T_C$ . We therefore conclude that the bcc-to-fcc paramagnetic phase transition is driven by the magnetic correlation energy.

In conclusion, we employed the GGA+DMFT many-body approach to compute the equilibrium crystal structure and phase stability of iron at the bcc-fcc transition. In particular, we found that the bcc-to-fcc structural phase transition occurs well above the magnetic transition, and that the *magnetic* correlation energy is essen-

tial to explain this *structural* transition in paramagnetic iron. The above result and those for the equilibrium lattice constant and the variation of the unit cell volume at the bcc-fcc phase transition agree well with experiment.

We thank J. Deisenhofer, Yu. N. Gornostyrev, F. Lechermann, A. I. Lichtenstein, M. I. Katsnelson, A. A. Katanin, K. Samwer, and V. Tsurkan for valuable discussions. Support by the Russian Foundation for Basic Research under Grant No. RFFI-07-02-00041, RFFI-08-02-91953, the Deutsche Forschungsgemeinschaft through SFB 484 in 2009 and TRR 80 as of January 1, 2010, is gratefully acknowledged.

- 
- [1] Z. S. Basinski, W. Hume-Rothery, and A. L. Sutton, Proc. R. Soc. London, Ser. A **229**, 459 (1955).
- [2] R. W. G. Wyckoff, Crystal structure, vol. 1 (Wiley, New York, 1963).
- [3] S. Y. Savrasov, Phys. Rev. Lett. **81**, 2570 (1998).
- [4] C. S. Wang, B. M. Klein, and H. Krakauer, Phys. Rev. Lett. **54**, 1852 (1985); J. M. MacLaren, D. P. Clougherty, and R. C. Albers, Phys. Rev. B **42**, 3205 (1990); D. Singh *et al.*, *ibid.* **44**, 7701 (1991).
- [5] J. P. Perdew, K. Burke, and M. Ernzerhof, Phys. Rev. Lett. **77**, 3865 (1996).
- [6] D. J. Singh, W. E. Pickett, and H. Krakauer, Phys. Rev. B **43**, 11628 (1991); L. Stixrude, R. E. Cohen, and D. J. Singh, *ibid.* **50**, 6442 (1994); A. Dal Corso and S. de Gironcoli, *ibid.* **62**, 273 (2000).
- [7] E. C. Stoner, Proc. R. Soc. London, Ser. A **169**, 339 (1939); G. L. Krasko and G. B. Olson, Phys. Rev. B **40**, 11536 (1989).
- [8] H. Hasegawa and D. G. Pettifor, Phys. Rev. Lett. **50**, 130 (1983).
- [9] V. I. Anisimov *et al.*, J. Phys.: Cond. Matt. **9**, 7359 (1997); A. I. Lichtenstein and M. I. Katsnelson, Phys. Rev. B **57**, 6884 (1998); K. Held *et al.*, Phys. Status Solidi B **243**, 2599 (2006); G. Kotliar *et al.*, Rev. Mod. Phys. **78**, 865 (2006).
- [10] W. Metzner and D. Vollhardt, Phys. Rev. Lett. **62**, 324 (1989); G. Kotliar and D. Vollhardt, Phys. Today **57**, No. 3, 53 (2004); M. I. Katsnelson *et al.*, Rev. Mod. Phys. **80**, 315 (2008).
- [11] A. I. Lichtenstein, M. I. Katsnelson, and G. Kotliar, Phys. Rev. Lett. **87**, 067205 (2001).
- [12] A. A. Katanin *et al.*, Phys. Rev. B **81**, 045117 (2010).
- [13] J. B. Goodenough, Phys. Rev. **120**, 67 (1960); V. Yu. Irkhin, M. I. Katsnelson, and A. V. Trefilov, J. Phys.: Cond. Matt. **5**, 8763 (1993).
- [14] I. Leonov *et al.*, Phys. Rev. Lett. **101**, 096405 (2008); I. Leonov *et al.*, Phys. Rev. B, **81**, 075109 (2010).
- [15] G. Trimarchi *et al.*, J. Phys.: Cond. Matt. **20**, 135227 (2008); Dm. Korotin, *et al.* Eur. Phys. J. B **65**, 91 (2008).
- [16] Calculations have been done using the PWSCF package: S. Baroni *et al.*, URL <http://www.pwscf.org>.
- [17] E. Antonides, E. C. Janse, and G. A. Sawatzky, Phys. Rev. B **15**, 1669 (1977); M. M. Steiner, R. C. Albers, and L. J. Sham, *ibid.* **45**, 13272 (1992); M. Cococcioni and S. de Gironcoli, *ibid.* **71**, 035105 (2005); I. Yang, S. Y. Savrasov, and G. Kotliar, Phys. Rev. Lett. **87**, 216405 (2001); J. Sánchez-Barriga *et al.*, *ibid.* **103**, 267203 (2009); N. L. Stojić and N. L. Binggeli, J. Magn. Magn. Matter. **320**, 100 (2008).
- [18] We note that using a double counting correction in the fully localized limit gives qualitatively the same results for the phase stability of paramagnetic Fe.
- [19] J. E. Hirsch and R. M. Fye, Phys. Rev. Lett **56**, 2521 (1986).
- [20] A complete calculation of the thermodynamic properties of Fe would also require the determination of the entropic contribution to the Gibbs free energy. The computation of electronic and lattice entropies from first principles is a great theoretical challenge which poses unsolved problems even in DFT. The inclusion of correlation effects makes the problem even more complex and therefore untractable even for state-of-the-art techniques. We note, however, that an explicit inclusion of the entropy terms would not even modify the qualitative features of the  $\alpha - \gamma$  phase transition obtained within our investigation, e.g., the result  $T_C < T_{\text{struct}}$ , for the following reason. The entropy change  $\Delta S$ , which may be determined from the slope of the  $\alpha - \gamma$  phase boundary at  $T_{\text{struct}}$  using the Clausius-Clapeyron equation, leads only to a small energy change of  $T\Delta S \sim 0.008$  eV/at. This is considerably smaller than the total energy change  $\Delta E \sim 0.02$  eV/at at  $T = 1.2 T_C$  (see Fig. 2). This finding is fully consistent with our result that it is the *magnetic correlation energy* which is the driving force behind the bcc-to-fcc paramagnetic phase transition.
- [21] K. I. Kugel and D. I. Khomskii, Sov. Phys. Usp. **25**, 231 (1982).
- [22] E. Knittle, in *Mineral Physics and Crystallography: A Handbook of Physical Constants*, edited by T. J. Ahrens (American Geophysical Union, Washington, DC, 1995); E. G. Moroni *et al.*, Phys. Rev. B **56**, 15629 (1997).
- [23] Neglecting the slight difference between the Fe  $t_{2g}$  and  $e_g$  occupancies, the Coulomb interaction part of the Hamiltonian (1) can be rewritten as  $\hat{H}_U = \frac{1}{2}\bar{U}\hat{N}^2 - \frac{1}{4}I\hat{m}_z^2$ , with an averaged Coulomb interaction  $\bar{U} \sim 0.75$  eV and exchange interaction  $I = \frac{1}{5}(U + 4J) \sim 1.08$  eV. Here  $\hat{N} = \sum_{m\sigma} \hat{n}_{im\sigma}$  and  $\hat{m}_z = \sum_m(\hat{n}_{im\uparrow} - \hat{n}_{im\downarrow})$  are operators of the total number of particles and magnetization, respectively. Therefore the Coulomb energy contribution to the total energy is proportional to the squared total number of particles and local moment,  $E_U = \frac{1}{2}\bar{U}\langle N^2 \rangle - \frac{1}{4}I\langle m_z^2 \rangle$ . Since  $\langle N^2 \rangle$  only weakly depends on the  $c/a$  distortion, the main dependence of the total energy of the paramagnetic phase on  $c/a$  is due to the magnetic correlation energy.